Desalination and Water Treatment
www.deswater.com

doi: 10.1080/19443994.2015.1118887

57 (2016) 23266–23272
October

Taylor & Francis
Taylor & Francis Group

Study of the influence of operational conditions and hollow-fiber diameter on the ultrafiltration performance of a secondary treatment effluent

M. Torà-Grau, J.L. Soler-Cabezas, M.C. Vincent-Vela*, J.A. Mendoza-Roca, F.J. Martínez-Francisco

Instituto de Seguridad Industrial, Radiofísica y Medio Ambiental Universitat Politècnica de València, Camino de Vera s/n 46022, Valencia, Spain, Tel. +34 96 387 70 00, ext. 76380; Fax: +34 96 387 76 39; emails: mitogr@etsii.upv.es (M. Torà-Grau), jsoca@isirym.upv.es (J.L. Soler-Cabezas), mavinve@iqn.upv.es (M.C. Vincent-Vela), jamendoz@iqn.upv.es (J.A. Mendoza-Roca), framarfr@iqn.upv.es (F.J. Martínez-Francisco)

Received 5 March 2015; Accepted 5 November 2015

ABSTRACT

Secondary treatment effluents from municipal wastewater treatment plants (MWWTP) must achieve high water quality standards for their reuse in agriculture. To achieve these standards, ultrafiltration (UF) process, which is economically feasible, is carried out. However, UF has a drawback, membrane fouling, which causes operating difficulties and an increment of the operating cost. In order to minimize this phenomenon, it is important to determine the best operational conditions. Wastewater samples provided by MWWTP have a lot of variability in their composition due to factors such as temperature, efficiency of the secondary treatment, etc. Besides, the soluble microbial products of the secondary effluent are dependent on the type of the biological treatment implemented and its operating conditions. A model wastewater feed solution was prepared consisting of 15 mg/L of bovine serum albumin and 5.5 mg/L of dextran. In this research, UF tests were performed with the optimal simulated wastewater using two membranes UFCM5 Norit X-flow® hollow-fiber: one of them with a fiber diameter of 1.5 mm and the other one with a fiber diameter of 0.8 mm. The operational conditions, which influence membrane fouling, were varied in the range of 62–100 kPa for transmembrane pressure (TMP) and in the range of 0.8–1.2 m/s for cross-flow velocity (CFV). The best operational conditions were selected in terms of higher permeate flux. The highest permeate flux was obtained for the membrane of 0.8 mm and the lower energy consumption was achieved at a CFV of 1.2 m/s and a TMP of 62 kPa.

Keywords: Ultrafiltration; Hollow-fiber diameter; Operational conditions; Secondary treatment effluent; Fouling

*Corresponding author.

Presented at EuroMed 2015: Desalination for Clean Water and Energy Palermo, Italy, 10–14 May 2015. Organized by the European Desalination Society.

1. Introduction

Nowadays, tertiary treatments are very important and necessary in order to improve the quality of the secondary treatment effluents (STEs). Many municipal wastewater treatment plants (MWWTP) use ultrafiltration (UF) as a tertiary treatment because it has been proved to be a reliable process.

There are many reasons to use UF as a tertiary treatment. For example, among the advantages of UF processes there can be found: the high quality of permeate, no by-product generation, the high efficiency achieved, the low energy consumed and the small footprint [1–5]. However, UF processes have an important drawback: membrane fouling [6]. As a consequence of that, the permeate flux decreases [7] and it causes an increment of operating and maintenance costs [7,8]. Therefore, the main objective of this work is to carry out a study on the influence of operational conditions on permeate flux.

The fouling caused by UF membranes could be caused by different fouling mechanisms. The fouling mechanisms, which are based on Hermia's model, are: complete pore blocking, the intermediate pore blocking, the standard pore blocking and gel layer. The difference among the fouling mechanisms is the way in which the solute has been deposited on the membrane surface. According to the literature, Field et al. [9] and Vincent Vela et al. [10], each Hermia's model assumes different hypotheses. The complete pore blocking model assumes that all solute molecule that arrives at the membrane surface participates in blocking, but no solute attaches onto a previously deposited one. The permeate flux through the no blocked pores remains constant, then the reduction in permeate flux is proportional to the reduction in membrane surface area. The intermediate pore blocking model explains that a membrane pore could not be blocked by a solute and the probability that a solute attached over a previously deposited solute is considered. In the intermediate pore blocking, the membrane surface that is not blocked diminishes with time. The standard pore blocking model assumes that solutes are deposited within the membrane pores and the pore volume is reduced with time. In this case, some molecules could be adsorbed instead of being only deposited over the internal surface of membrane pores. Finally, the gel layer model assumes that solutes cannot enter inside the membrane pores and they form a gel layer over the membrane surface.

Soluble microbial products (SMP) constitute the majority of the organic compounds of the secondary effluents [11]. Besides SMP, refractory NOM coming from drinking water and synthetic organic compounds at very low concentrations as personal care products and pharmaceutical compounds. Although the role of SMP is still being investigated, its contribution to the membrane fouling has been reported by a great number of authors ([12–16]). In order to mimic the predominant substances in SMP, authors have used different polysaccharides and proteins. These compounds were previously reported to be used by other authors as Nataraj et al. [17] and Nguyen [18] to simulate STE wastewaters. STEs UF performance is well reproduced by binary mixtures of protein/polysaccharides consisting of bovine serum albumin (BSA) and dextran [9,12,13].

There are three factors which are the main factors responsible for membrane fouling: the membrane material properties, the feed characteristics and the operating parameters. Irreversible fouling can be due to the interactions among solvent, solute and membrane. In order to understand the fouling phenomena it is important to know the interactions between membrane-solute and between solute-solute. The first interaction explains the fouling through the adsorption of solute on the membrane surface. This interaction will modify the particle deposition and pore blocking mechanisms. The interaction between solute and solute cause an aggregation of solutes on the surface, which can be adsorbed previously by other solutes [19,20].

In this work, two operating parameters, transmembrane pressure (TMP) and cross-flow velocity (CFV), and two types of hollow fiber membranes of different fiber diameter were analyzed to evaluate their influence on membrane fouling. For this purpose, a model wastewater feed solution, capable of representing the STE performance, was used to ensure that the feed wastewater composition was the same for all the experiments. The best operational conditions to minimize membrane fouling during UF tests were selected.

2. Materials and methods

2.1. Model wastewater composition

The model wastewater was prepared according to the results from a previous work [21]. In that work, the optimal model wastewater to simulate the STE composition consisted of 15 mg/L of BSA and 5.5 mg/L of dextran.

The protein used to simulate STE composition was BSA from Sigma–Aldrich and the carbohydrate used was dextran (250,000 Da from VWR International Ltd). Both of them were dissolved with tap water and with a gentle stirring. It is important to note that BSA may form aggregates, increasing its particle size [22].

Once the model wastewater was prepared, its composition was compared to that of the STE in terms of proteins, carbohydrates and chemical oxygen demand (COD). Protein concentration was determined by MicroBCA assay from Applichem, carbohydrate concentration was determined by the *anthrone* method from Panreac and COD was determined using kits from Merck.

The initial experiments were carried out both with STE and simulated wastewater (SW) in order to check that model solutions mimic properly STE.

2.2. Hollow-fiber membranes

To carry out UF tests, hollow-fiber membranes were selected because they are the best membranes for the treatment of STE according to the literature [20,23,24].

The advantages of hollow fiber membranes, over flat sheet membranes, are: high active surface/volume ratio [25], the productivity per membrane module is higher [26] and they have self mechanical support, flexibility and easy handling [27].

Two hollow-fiber membranes were used, both from Norit X-flow. The main characteristics of these membranes are shown in Table 1.

2.3. Lab-scale plant and operational conditions

The lab-scale plant used to perform the UF tests was Norit X-flow T/RX-300. During the UF tests the feed solution was stirred and a temperature regulator was used to keep the temperature constant. Data were logged in a programmable logic controller (PLC). Besides, the retentate and the permeate were both returned to the feed tank and the permeate flux was monitored.

The experimental conditions were selected according to previous literature: low TMPs between 62 and 100 kPa [28] and CFVs between 0.8 and 1.2 m/s [29,30].

Table 1
Main characteristics of the hollow-fiber membranes

Molecular weight cut-off (MWCO)	200,000 Da
Material	Polyethersulfone/ polyvinylpyrrolidone (PES/PVP)
Configuration	Inside-out
Diameter	0.8/1.5 mm
Active area	0.07/0.04 m^2

2.4. Cleaning protocol

The cleaning protocol, three steps, was performed at the lowest TMP and the highest CFV achieved in the lab-scale plant. The first step consisted of a rinse with deionized water during 30 min at 25°C. The second step was a chemical cleaning performed at 40°C using 154 ppm of NaClO and 0.5 mol/L of NaOH in deionized water. The third step was rinsing at the same experimental conditions of the first step. The hydraulic permeability was evaluated after each cleaning protocol to ensure that initial membrane permeability was restored.

2.5. Flux normalization

As the permeabilities after each UF test were not completely restored, permeate flux was normalized according to Eq. (1):

$$J_{\mathrm{N}} = J \cdot \frac{R_0}{R_{\mathrm{m}}} \tag{1}$$

In Eq. (1) J is the permeate flux obtained during the test, J_{N} is the normalized permeate flux, R_0 is the resistance of the membrane before its first use and R_{m} is the membrane resistance before each test.

3. Results and discussion

In Figs. 1 and 2 the permeate flux decline with time for the STE and the SW at the same experimental conditions are compared for the two membranes used. It can be observed that the SW represents well the STE UF performance for both membranes.

The permeate flux decline with time for the two hollow-fiber membranes with different fiber diameter is compared for four different experimental conditions (Figs. 3–6). The results showed that the membrane with a fiber diameter of 0.8 mm was the one that achieved the highest permeate fluxes (lowest membrane fouling) for all the experimental conditions tested.

The highest percentage differences in long term permeate flux between both membranes were 67%. The highest steady-state permeate flux achieved for the membrane with a fiber diameter of 1.5 mm is approximately 50 L/m^2 h, whereas in the case of the membrane with a fiber diameter of 0.8 mm it is around 150 L/m^2 h. These results are in accordance with those obtained by Mondor et al. [31]. They worked with three different fiber diameters and they

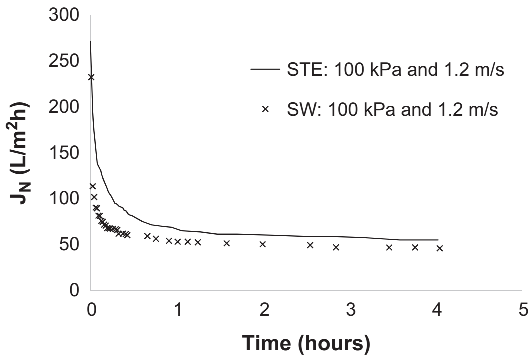

Fig. 1. Permeate flux decline vs. time with a hollow-fiber diameter of 1.5 mm.

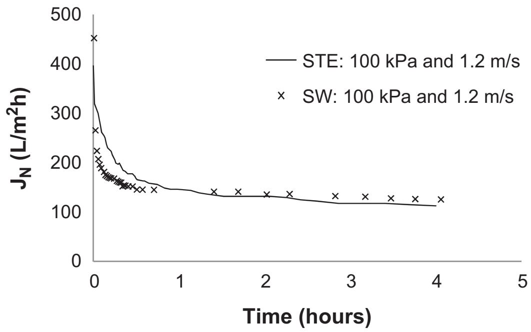

Fig. 2. Permeate flux decline vs. time with a hollow-fiber diameter of 0.8 mm.

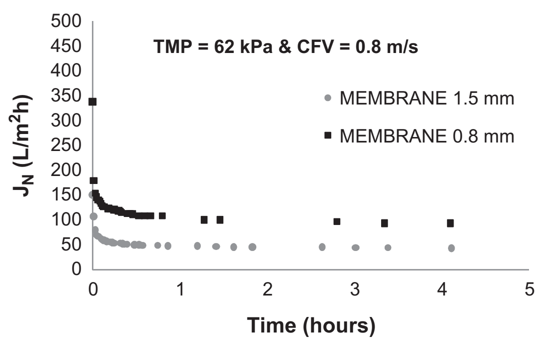

Fig. 3. Permeate flux decline vs. time with SW at 62 kPa and 0.8 m/s.

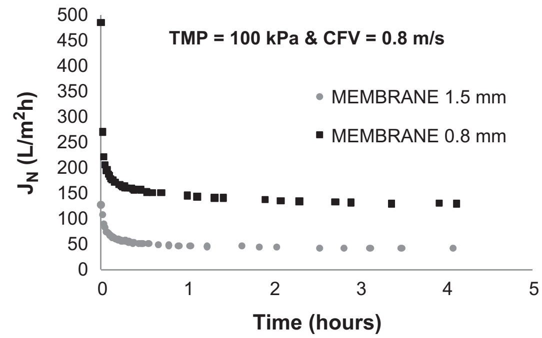

Fig. 4. Permeate flux decline vs. time with SW at 100 kPa and 0.8 m/s.

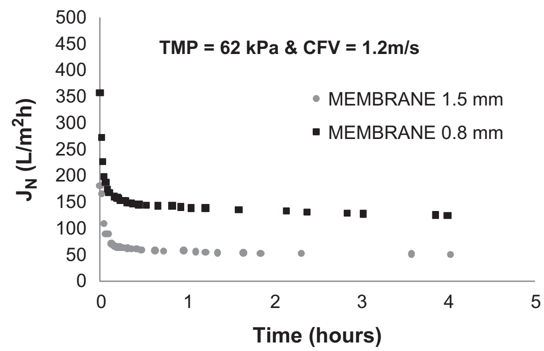

Fig. 5. Permeate flux decline vs. time with SW at 62 kPa and 1.2 m/s.

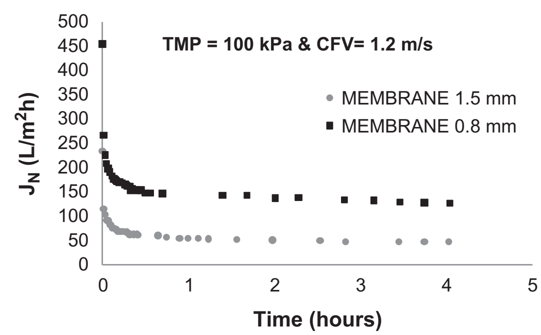

Fig. 6. Permeate flux decline vs. time with SW at 100 kPa and 1.2 m/s.

concluded that the membrane with the smallest diameter achieved the highest permeate flux. As well, Chang and Fane [32] studied the effect of fiber diameter on flux decline and they concluded that the fiber with the highest diameter tested produced more flux decline. This fact is also satisfied in the present work, in which the membrane with a fiber diameter of 1.5 mm produced a 71.2% of flux decline and the membrane with a fiber diameter of 0.8 mm declined the flux in a 64.4%.

Once the membrane was selected, the influence of TMP and CFV on permeate flux for this membrane

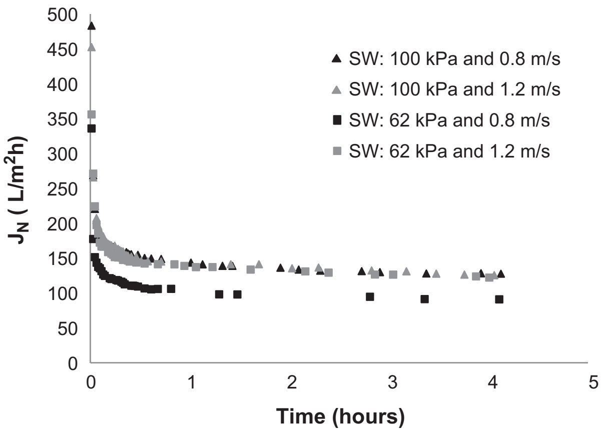

Fig. 7. Permeate flux decline vs. time with the membrane of 0.8 mm of diameter.

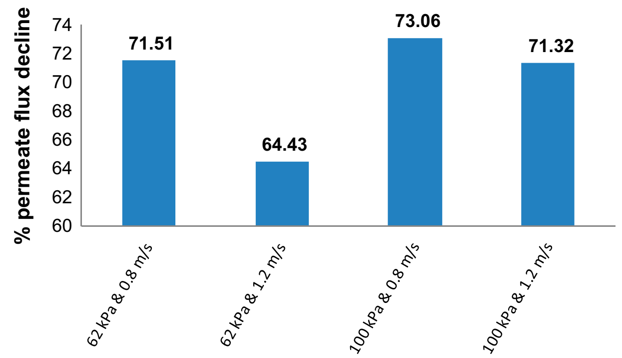

Fig. 8. Percentage of permeate flux decline for each operating condition.

was studied (Fig. 7). The worst result in terms of permeate flux is obtained for 62 kPa and 0.8 m/s. There were not significant differences in permeate flux for the rest of experimental conditions tested. Therefore, the optimal experimental conditions were selected on the basis of the lowest energy consumption (for the same flux, the operating conditions of lower pressure and lower CFV may be selected). This fact is achieved in the case of lowest TMP (62 kPa) and at a CFV of 1.2 m/s.

Fig. 8 shows the values of permeate flux decline for each experimental condition tested in terms of percentage of steady-state permeate flux with respect to the initial permeate flux. It can be seen that the test performed at 62 kPa and 1.2 m/s was the test that presented the lowest permeate flux decline. This fact indicated that the fouling produced for these operational conditions was the lowest.

Briefly, Figs. 3–6 show the flux decline over the time at different experimental conditions for each membrane (with different diameter). The results indicate that the membrane with a diameter of 0.8 mm has a higher steady-state flux, so the fouling produced is lower than in the case of the membrane of 1.5 mm of diameter. Fig. 3 (62 kPa and 0.8 m/s) shows the worst results because the steady-state flux for the membrane of 0.8 mm of diameter was lower than the other figures. Among the other figures, the best experimental condition selected is a pressure of 62 kPa and a CFV of 1.2 m/s because the pressure is lower and then the energy consumption could be lower too.

It is known that UF operating conditions have an important effect on irreversible fouling of the UF membrane, which is caused mainly by natural organic matter (or EfOM). At higher pressures, the EfOM may penetrate into the membrane pores more easily and in addition the higher pressure may have mechanical effects on particles facilitating the particles to penetrate into pores of similar size. Moreover, higher pressures may compact the filtra-

Table 2
Proteins and carbohydrates rejection

Membrane (mm)	Experimental conditions	Proteins (%)	Carbohydrates (%)
1.5	62 kPa and 1.2 m/s	89.8	38.0
1.5	62 kPa and 0.8 m/s	78.8	33.0
1.5	100 kPa and 1.2 m/s	69.1	34.5
1.5	100 kPa and 0.8 m/s	68.9	42.0
0.8	62 kPa and 1.2 m/s	88.3	46.2
0.8	62 kPa and 0.8 m/s	81.6	40.8
0.8	100 kPa and 1.2 m/s	93.1	40.5
0.8	100 kPa and 0.8 m/s	92.3	44.7

tion cake [33]. Then, low pressures are preferred to high pressures.

Table 2 shows the proteins and carbohydrates rejection for the UF tests carried out with both membranes for all the experimental conditions considered in this study. These results were analyzed to evaluate the permeate quality. In terms of carbohydrates rejection, the UF test performed with the membrane of 0.8 mm, at 62 kPa and 1.2 m/s, achieved the highest value (46.16%). For proteins rejection, the test with the highest rejection value (93.15%) was that performed with the membrane of 0.8 mm of fiber diameter at 100 kPa and 1.2 m/s. However, the test carried out at 62 kPa and 1.2 m/s, for the same membrane, achieved a protein rejection of 88.35%, only 4.81% far from the maximum, what can be considered as negligible. On the other hand, the COD rejection was also evaluated and its values were in the range of 56.5–70.9%. In general terms, it can be stated that the highest rejection values corresponded with the membrane of 0.8 mm, what can be explained since its permeate flux was higher than that measured for the 1.5 mm membrane.

Considering the highest permeate flux, the lowest energy consumption and the high permeate quality, it can be concluded that the optimal operating conditions were achieved for the 0.8 mm membrane at a TMP of 62 kPa and a CFV 1.2 m/s.

4. Conclusions

The main objective of this research was to select the best operating conditions (TMP, CFV and hollow fiber diameter) to reduce the membrane fouling and energy consumption during STE UF. At the same time, it was necessary to achieve a high permeate quality. The analysis of all these factors allowed the selection of the optimal operating conditions: a membrane of 0.8 mm of fiber diameter, a TMP of 62 kPa and a CFV 1.2 m/s.

Acknowledgements

The authors of this work wish to gratefully acknowledge the financial support from the Generalitat Valenciana through the program "Ayudas para la realización de proyectos I+D para grupos de investigaciónemergentes GV/2013/126".

Symbols

J	—	permeate flux (L/m^2 h)
J_N	—	normalized permeate flux (L/m^2 h)
R_0	—	resistance of the membrane before the first use (m^{-1})
R_m	—	resistance of the membrane before each test (m^{-1})
μ	—	dynamic viscosity of the water (Pa s)
TMP	—	transmembrane pressure (kPa)
CFV	—	cross-flow velocity (m/s)
STE	—	secondary treatment effluent
SW	—	simulated wastewater
MWWTP	—	municipal wastewater treatment plant
UF	—	ultrafiltration
EPS	—	extracellular polymeric substances
BSA	—	bovine serum albumin
COD	—	chemical oxygen demand (mg/L)
MWCO	—	molecular weight cut-off
EfOM	—	effluent organic matter

References

[1] J.-J. Qin, M.H. Oo, H. Lee, R. Kolkman, Dead-end ultrafiltration for pretreatment of RO in reclamation of municipal wastewater effluent, J. Membr. Sci. 243 (2004) 107–113.

[2] J. Arévalo, G. Garralón, F. Plaza, B. Moreno, J. Pérez, M.Á. Gómez, Wastewater reuse after treatment by tertiary ultrafiltration and a membrane bioreactor (MBR): A comparative study, Desalination 243 (2009) 32–41.

[3] K. Katsoufidou, S.G. Yiantsios, A.J. Karabelas, An experimental study of UF membrane fouling by humic acid and sodium alginate solutions: The effect of backwashing on flux recovery, Desalination 220 (2008) 214–227.

[4] S. Muthukumaran, D.A. Nguyen, K. Baskaran, Performance evaluation of different ultrafiltration membranes for the reclamation and reuse of secondary effluent, Desalination 279 (2011) 383–389.

[5] R.K. Henderson, N. Subhi, A. Antony, S.J. Khan, K.R. Murphy, G.L. Leslie, V. Chen, R.M. Stuetz, P. Le-Clech, Evaluation of effluent organic matter fouling in ultrafiltration treatment using advanced organic characterisation techniques, J. Membr. Sci. 382 (2011) 50–59.

[6] S. Muthukumaran, J.V. Jegatheesan, K. Baskaran, Comparison of fouling mechanisms in low-pressure membrane (MF/UF) filtration of secondary effluent, Desalin. Water Treat. 52 (2014) 650–662.

[7] C.-H. Yu, L.-C. Fang, S.K. Lateef, C.-H. Wu, C.-F. Lin, Enzymatic treatment for controlling irreversible membrane fouling in cross-flow humic acid-fed ultrafiltration, J. Hazard. Mater. 177 (2010) 1153–1158.

[8] M.A. Saad, Early discovery of RO membrane fouling and real-time monitoring of plant performance for optimizing cost of water, Desalination 165 (2004) 183–191.

[9] R.W. Field, D. Wu, J.A. Howell, B.B. Gupta, Critical flux concept for microfiltration fouling, J. Membr. Sci. 100 (1995) 259–272.

[10] M.C. Vincent Vela, S. Álvarez Blanco, J. Lora García, E. Bergantiños Rodríguez, Analysis of membrane pore blocking models adapted to crossflow ultrafiltration in the ultrafiltration of PEG, Chem. Eng. J. 149 (2009) 232–241.
[11] D.J. Barker, D.C. Stuckey, A review of soluble microbial products (SMP) in wastewater treatment systems, Water Res. 33 (1999) 3063–3082.
[12] Z.-P. Wang, T. Zhang, Characterization of soluble microbial products (SMP) under stressful conditions, Water Res. 44 (2010) 5499–5509.
[13] S. Liang, C. Liu, L. Song, Soluble microbial products in membrane bioreactor operation: Behaviors, characteristics, and fouling potential, Water Res. 41 (2007) 95–101.
[14] Y. Shen, W. Zhao, K. Xiao, X. Huang, A systematic insight into fouling propensity of soluble microbial products in membrane bioreactors based on hydrophobic interaction and size exclusion, J. Membr. Sci. 346 (2010) 187–193.
[15] Y. Tian, Z. Li, Y. Ding, Y. Lu, Identification of the change in fouling potential of soluble microbial products (SMP) in membrane bioreactor coupled with worm reactor, Water Res. 47 (2013) 2015–2024.
[16] J.R. Pan, Y. Su, C. Huang, Characteristics of soluble microbial products in membrane bioreactor and its effect on membrane fouling, Desalination 250 (2010) 778–780.
[17] S. Nataraj, R. Schomäcker, M. Kraume, I.M. Mishra, A. Drews, Analyses of polysaccharide fouling mechanisms during crossflow membrane filtration, J. Membr. Sci. 308 (2008) 152–161.
[18] F.A.R.S.T. Nguyen, Chemical cleaning of ultrafiltration membrane fouled by an activated sludge effluent, Desalin. Water Treat. 34 (2011) 94–99.
[19] M. Zator, M. Ferrando, F. López, C. Güell, Membrane fouling characterization by confocal microscopy during filtration of BSA/dextran mixtures, J. Membr. Sci. 301 (2007) 57–66.
[20] K. Xiao, X. Wang, X. Huang, T.D. Waite, X. Wen, Analysis of polysaccharide, protein and humic acid retention by microfiltration membranes using Thomas' dynamic adsorption model, J. Membr. Sci. 342 (2009) 22–34.
[21] K.-J. Hwang, Y.-C. Chiang, Comparisons of membrane fouling and separation efficiency in protein/polysaccharide cross-flow microfiltration using membranes with different morphologies, Sep. Purif. Technol. 125 (2014) 74–82.
[22] M. Torà-Grau, J.L. Soler-Cabezas, M.C. Vincent-Vela, J.A. Mendoza-Roca, F.J. Martínez-Francisco, Comparison of different model solutions to simulate membrane fouling in the ultrafiltration of a secondary effluent from a municipal wastewater treatment plant, Desalin. Water Treat. 55(11) (2015) 2924–2930.
[23] S. Delgado, F. Díaz, L. Vera, R. Díaz, S. Elmaleh, Modelling hollow-fibre ultrafiltration of biologically treated wastewater with and without gas sparging, J. Membr. Sci. 228 (2004) 55–63.
[24] L. Fan, T. Nguyen, F.A. Roddick, J.L. Harris, Low-pressure membrane filtration of secondary effluent in water reuse: Pre-treatment for fouling reduction, J. Membr. Sci. 320 (2008) 135–142.
[25] D. Xiao, W. Li, S. Chou, R. Wang, C.Y. Tang, A modeling investigation on optimizing the design of forward osmosis hollow fiber modules, J. Membr. Sci. 392–393 (2012) 76–87.
[26] P.Z. Çulfaz, E. Rolevink, C. van Rijn, R.G.H. Lammertink, M. Wessling, Microstructured hollow fibers for ultrafiltration, J. Membr. Sci. 347 (2010) 32–41.
[27] F. Tasselli, A. Cassano, E. Drioli, Ultrafiltration of kiwifruit juice using modified poly(ether ether ketone) hollow fibre membranes, Sep. Purif. Technol. 57 (2007) 94–102.
[28] Y. Kaya, H. Barlas, S. Arayici, Evaluation of fouling mechanisms in the nanofiltration of solutions with high anionic and nonionic surfactant contents using a resistance-in-series model, J. Membr. Sci. 367 (2011) 45–54.
[29] F. Tasselli, A. Cassano, E. Drioli, Ultrafiltration of kiwifruit juice using modified poly(ether ether ketone) hollow fibre membranes, Sep. Purif. Technol. 57 (2007) 94–102.
[30] E.B.-R. M.C. Vincent-Vela, S. Alvarez-Blanco, J. Lora-Garcia, Estimation of the gel layer concentration in ultrafiltration: Comparison of different methods, Desalin. Water Treat. 3 (2009) 157–161.
[31] M. Mondor, O. Tuyishime, H. Drolet, Production of pea protein concentrates by ultrafiltration: Influence of hollow-fibre module, Innovative Food Sci. Emerg. Technol. 14 (2012) 135–138.
[32] S. Chang, A. Fane, The effect of fibre diameter on filtration and flux distribution—Relevance to submerged hollow fibre modules, J. Membr. Sci. 184 (2001) 221–231.
[33] G.F. Crozes, J.G. Jacangelo, C. Anselme, J.M. Laîné, Impact of ultrafiltration operating conditions on membrane irreversible fouling, J. Membr. Sci. 124 (1997) 63–76.